Left Atrium Right Atrium Network (LARANet): A Deep Neural Network for Biatrial Segmentation from MRI and CT Images

Rebecca A. Yu [1], Rheeda L. Ali PhD [2], Pallavi Pandey MD [2,3], Ryan P. Bradley PhD [2], David D. Spragg MD FHRS [3], Hugh G. Calkins MD FHRS [3], Natalia A. Trayanova PhD FHRS [1,2,4]

[1] Department of Biomedical Engineering, Johns Hopkins University, [2] Alliance for Cardiovascular Diagnostic and Treatment Innovation, [3] Division of Radiology, Department of Medicine, Johns Hopkins University, [4] Division of Cardiology, Department of Medicine, Johns Hopkins University

Objective

CLINICAL MOTIVATION

- Structural remodeling in the left and right atrium (LA, RA) significantly impacts the success rates of catheter ablation in patients with Persistent Atrial Fibrillation (PsAF)
- Atrial anatomy reconstruction and quantification of fibrotic substrate is clinically important for guiding catheter ablation
- Atrial segmentation is the crucial first step of substrate quantification, but it currently presents as a bottleneck in the pipeline as it needs to be done manually

TECHNICAL MOTIVATION

- Variable atrial anatomy and thin atrial walls, compounded with poor and inconsistent image quality, lead to low generalizability in many segmentation neural network (NN) models that only focus on LA segmentation

BACKGROUND

- State-of-the-art NNs implement a two-step process:
  1. A region-of-interest (ROI) NN to identify a biatrial bounding box, followed by
  2. An atrial segmentation (ASeg) NN for refined epicardial segmentation
- This two-step process means that outcomes of the second ASeg NN are heavily dependent on the accuracy of predictions from the ROI NN

AIM - Define and implement a biatrial segmentation NN that successfully segments LA and RA of never-before-seen clinical images with high anatomical anatomical consistncy

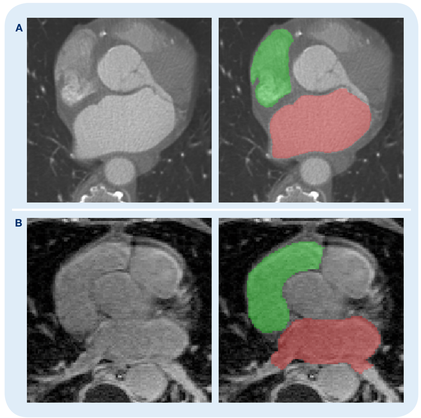

Fig 1. Clinical cardiac image modalities (left) that are consequently segmented (right, LA = red, RA = green) for substrate quantification. **(A)** computed tomography (CT) cardiac scan **(B)** late-gadolinium enhanced magnetic resonance imaging (LGE-MRI).

Methods

NEURAL NETWORK DEVELOPMENT & STRUCTURE

- Developed a 2-stage 3D NN (LARANet) that first identifies the atrial ROI then refines the atrial segmentation using a U-Net structure defined in Ronneberger et al.
- Added custom loss functions and image pre-processing to constrain ROI bounding boxes to appropriate atrial regions
- Added a discriminator as validated by Isola, et al. to classify predictions as either real or fake in order to penalize unrealistic but otherwise “optimal” predictions
- Overall, the structure of the network is:
  1. ROI identification NN which identifies a biatrial bounding box atrial prediction (P-ROI)
  2. Atrial segmentation (ASeg) refinement NN which accepts the output from ROI-NN to refine the epicardial segmentation for a final ASeg prediction (P-ASEG)
  3. Prediction discriminator which will determine the “realistic-ness” of generated segmentations for the networks to optimize on

LOSS FUNCTIONS & ROI CONSTRAINTS

- The base loss function averaged the Hausdorff Dice loss (DL) and binary cross entropy loss (BL)
- ROI loss (RL) was defined to be a weighted summation of:
  1. Volumetric difference between the GT ROI and P-ROI bounding boxes
  2. Pixel-wise distance of the centers of mass (CoM) between GT ROI and P-ROI
  3. Difference between CoM to bounding box midpoint distances for GT ROI and P-ROI
- The ROI bounding box is further constrained by a proportion-based erosion-dilation to ensure extra-cardiac structures are excluded

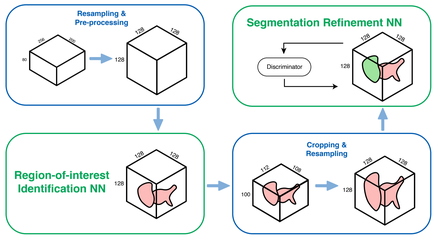

Fig 2. Overview of NN structure. The main parts of the NN are (1) a ROI identification NN, (2) an atrial segmentation (ASeg) refinement NN, (3) prediction discriminator for the ASeg NNs as an anatomical correction GAN.

MODEL TRAINING & EVALUATION

- Each NN model was trained through grid testing to find the optimal set of hyperparameters
  - Parameters optimized: learning rate, momentum, loss beta, discriminator weight, receptive field size
- The ROI NN model was trained with and without RL
- Resulting P-ROIs were used as input for training the ASEG NN after bounding box constraints are applied
- To generate the final output, P-ASegs are resampled back to the original spacing and dimensions
- Final resampled outputs were evaluated using Sørensen–Dice coefficient (DC) and Hausdorff distance (HD)

Results

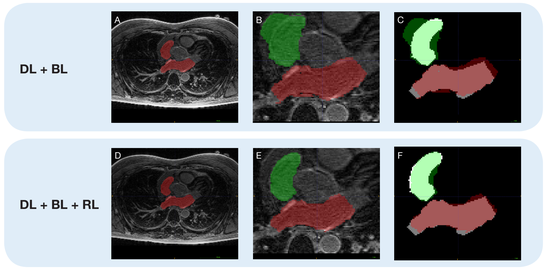

Fig 3. Visual comparison of NN segmentation results for a LGE-MRI image stack. **(A)** Output of ROI NN without ROI loss (RL) - segmentation pixels used to define bounding box. **(B)** Output of ASeg NN without RL- left atrium (LA) and right atrium (RA) predictions, shown in red and green respectively, overlain on top of cropped LGE-MRI slice. **(C)** Output of ASeg NN without RL (LA and RA predictions) overlain on top of ground truth LA and RA segmentations, shown in white and grey respectively. **(D)** Output of ROI NN without ROI loss (RL) - segmentation pixels used to define bounding box. **(E)** Output of ASeg NN with RL- LA and RA segmentations overlain on top of cropped LGE-MRI slice. **(F)** Output of ASeg NN with RL (LA and RA predictions) overlain on top of ground truth LA and RA segmentations.

RESULTING METRICS

	ROI NN			ASeg NN	
	Avg DC	Avg HD	Absolute Volume Difference (pixels)	Avg DC	Avg HD
DL + BL	0.9313 ± 0.04	6.1744 ± 8.37	9472 ± 73120	0.9333 ± 0.03	15.035 ± 12.36
DL + BL + RL	0.9351 ± 0.04	5.8310 ± 7.86	8832 ± 68100	0.9427 ± 0.02	13.88 ± 8.34

SIGNIFICANCE

- ROI NN with RL, DL, and BL resulted in higher Dice Coefficients (DC) (p=0.29, ns), smaller HDs (p=0.32, n.s.), and smaller volume deviations from GT (p=0.31, ns) than those trained with only DL and BL. Models trained with RL have lower standard deviations and fewer outliers for P-ROI.
- P-ASeg consequently also had significantly higher DCs (p=.004) and smaller HDs (p=0.05, n.s.) when trained from the P-ROI with RL. Differences in standard deviation are significant for DC (p=0.04), but not HD (p=0.25) when comparing the ASeg NN trained with RL, DL, and BL to a model with DL and BL only.
- Note that Hausdorff distance appears worse in the ASeg because metrics are evaluated on images that are cropped then resampled. This causes a significant change in the metrics derived as Hausdorff calculates distance by pixels. When looking at segmentations with DL + BL + RL, it is evident that adding in RL significantly improves adherence to anatomical guidelines.

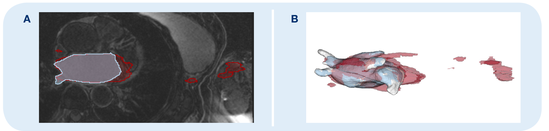

Fig 4. Comparison of LA ROI identification with RL + ROI-constraining image processing (blue) and without RL + ROI-constraining image processing (red). **(A)** Visualization in the atrial view shows the network without RL + ROI-constraining image processing oversegmenting the LA and falsely segmenting extracardiac structures on the right. **(B)** Visualization through a 3D model view illustrates how the network without RL or ROI-constraining image processing overpredicts and generates an output that does not conform to anatomical constraints.

BENCHMARK LA SEGMENTATION (LGE-MRI) METRICS

	Avg DC	Max DC	Min DC	Avg HD	Min HD	Max HD
BENCHMARK (CHEN ET AL.)	0.9151 ± 0.03	0.962	0.832	15.46 ± 18.11	5.08	107.94
LARANet	0.9177 ± 0.03	0.964	0.821	12.87 ± 4.59	6.15	29.08

3D VIEW

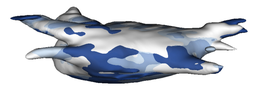

GT
LARANet
Benchmark

ATRIAL VIEW

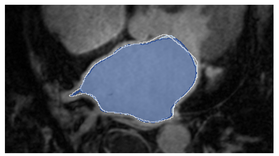

LARANet and Benchmark segmentations both adhere to anatomical constraints and appropriately segment the LA.

CORONAL VIEW

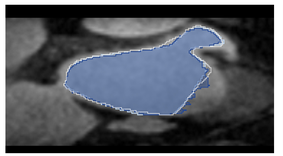

LARANet and Benchmark segmentations both identify the correct LA region; however, the Benchmark segmentation is jagged along the bottom right, failing to adhere to anatomical constraints.

SAGITTAL VIEW

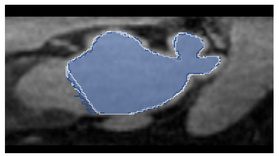

LARANet, and Benchmark segmentations both identify the correct LA region; however, the Benchmark segmentation is jagged along the bottom left, failing to adhere to anatomical constraints.

LA + RA SEGMENTATION (NEVER-BEFORE-SEEN IMAGES, LGE-MRI + CT) METRICS

	Avg DC	Max DC	Min DC	Avg HD	Min HD	Max HD
LA	0.9300 ± 0.03	0.974	0.851	15.68 ± 8.82	1.77	117.46
RA	0.895 ± 0.03	0.964	0.499	19.96 ± 11.60	1.88	157.67

Discussion

- Accurate segmentation of clinical images is key in anatomical reconstruction of atrial anatomy and the quantification of fibrotic substrate
- Manual segmentation of cardiac images is time-consuming and tedious (taking up to 8 hours), but current state-of-the-art NNs generate segmentations that lack spatial consistency
- The combination of RL and ROI-constraining image processing leads segmentations to appropriately segment atrial structures in the appropriate cardiac region
- LARANet successfully segments both the LA and RA of never-before-seen clinical cardiac images (both LGE-MRI and CT) with an average biatrial DC of 0.926 ± 0.024. LARANet improves the performance of atrial segmentation NNs by maintaining anatomical consistency and it’s biatrial approach also has promising applications in both clinical practice and future research.
- Next steps: Implement LARANet in clinical pipelines to evaluate the significance of LARANet vs manual segmentations

References

1. Andrade J., Khairy P., Dobrev D., Nattel S. (2014). The clinical profile and pathophysiology of atrial fibrillation: relationships among clinical features, epidemiology, and mechanisms. Circ. Res. 114 1453–1468. 10.1161/CIRCRESAHA.114.303211
2. Boyle, P.M., Zghaib, T., Zahid, S. et al. Computationally guided personalized targeted ablation of persistent atrial fibrillation. Nat Biomed Eng 3, 870–879 (2019). https://doi.org/10.1038/s41551-019-0437-9
3. Trayanova, N. A. (2014). Mathematical Approaches to Understanding and Imaging Atrial Fibrillation. Circulation Research, 114(9), 1516-1531. doi:10.1161/circresaha.114.302240
4. Boyle, P. M., Hakim, J. B., Zahid, S., Franceschi, W. H., Murphy, M. J., Prakosa, A., . . . Trayanova, N. A. (2018). The Fibrotic Substrate in Persistent Atrial Fibrillation Patients: Comparison Between Predictions From Computational Modeling and Measurements From Focal Impulse and Rotor Mapping. Frontiers in Physiology, 9. doi:10.3389/fphys.2018.01151
5. Zheng, Q., Delingette, H., Duchateau, N., & Ayache, N. (2018). 3-D Consistent and Robust Segmentation of Cardiac Images by Deep Learning With Spatial Propagation. IEEE Transactions on Medical Imaging, 37(9), 2137-2148. doi:10.1109/tmi.2018.2820742
6. Isola, P., Zhu, J., Zhou, T., & Efros, A. A. (2017). Image-to-Image Translation with Conditional Adversarial Networks. 2017 IEEE Conference on Computer Vision and Pattern Recognition (CVPR). doi:10.1109/cvpr.2017.632
7. Ronneberger O, Fischer P and Brox T, U-Net: Convolutional Networks for Biomedical Image Segmentation Medical Image Computing and Computer-Assisted Intervention – MICCAI 2015; 2015: 234-241.

Disclosure Nothing to disclose, no conflicting interests.